Biochemistry

Subscriber access provided by University of South Dakota

Article

Crystal structures of Candida albicans phosphodiesterase-2 and implication on its biological functions

Ting Yao, Yiyou Huang, Meng Zhang, Yujuan Chen, Hairun Pei, Jianyou Shi, Huanchen Wang, Yousheng Wang, and Hengming Ke

Biochemistry, **Just Accepted Manuscript** • DOI: 10.1021/acs.biochem.8b00707 • Publication Date (Web): 19 Sep 2018

Crystal structures of *Candida albicans* phosphodiesterase-2 and implication on its biological functions

Ting Yao[1,§], Yiyou Huang[2,§,¶], Meng Zhang[1], Yujuan Chen[1], Hairun Pei[1], Jianyou Shi[2,4,*], Huanchen Wang[3,*], Yousheng Wang[1,*], Hengming Ke[2,*]

1 Beijing Advanced Innovation Center for Food Nutrition and Human Health, Beijing Technology and Business University, Beijing 100048, China
2 Department of Biochemistry and Biophysics and Lineberger Comprehensive Cancer Center, The University of North Carolina, Chapel Hill, NC 27599-7260, USA
3 Laboratory of Signal Transduction, NIEHS/NIH, 111 Alexander Drive, Research Triangle Park, NC, 27709, USA
4 Individualized Medication Key Laboratory of Sichuan Province, Sichuan Academy of Medical Science & Sichuan Provincial People's Hospital, School of Medicine, University of Electronic Science and Technology of China, Chengdu, Sichuan, China, 610072

Running title: Crystal structure of caPDE2

* Correspondence should be addressed to H. Ke, Tel: +1-919-966-2244, fax: +1-919-966-2852, email: hke@med.unc.edu, Y. Wang, Tel: 86-10-6898-4905, email: wangys@th.btbu.edu.cn, or J. Shi, email: shijianyoude@126.com.

¶ Present address:
School of Pharmaceutical Sciences, Sun Yat-Sen University, Guangzhou 510006, P. R. China

Keywords: phosphodiesterase, yeast, crystal structure, second messenger cAMP, enzymatic kinetics.
Abbreviations: PDEs, phosphodiesterase; cGMP, guanosine 3', 5'-monophosphate; cAMP, adenosine 3', 5'-monophosphate.

Abstract

The cAMP signaling system plays important roles in the physiological processes of pathogen yeast *Candida albicans*, but its functional mechanism has not been well illustrated. Here, we report the enzymatic characterization and crystal structures of *Candida albicans* phosphodiesterase 2 (caPDE2) in the unliganded and IBMX complexed forms. CaPDE2 is a monomer in liquid and crystal states and specifically hydrolyzes cAMP with K_M of 35 nM. It does not effectively hydrolyze cGMP as shown by $1.32x10^5$ fold specificity of cAMP/cGMP. The crystal structure of caPDE2 shows significant differences from those of human PDEs. First, the N-terminal fragment of caPDE2 (residues 1-201) tightly associates with the catalytic domain to form a rigid molecular entity, implying its stable molecular conformation for *Candida albicans* to resist environmental stresses. Second, the M-loop, a critical fragment for binding of substrate and inhibitors to human PDEs, is not a part of the caPDE2 active site. This feature of caPDE2 may provide structure basis for design of selective inhibitors for treatment of yeast infection.

Table of Content graphic

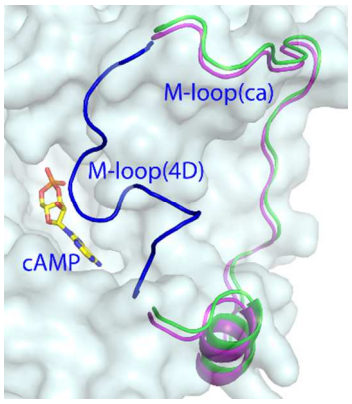

Dramatic conformation difference between the M-loops of yeast caPDE2 and PDE4D.

Introduction

Candida albicans is an opportunistic pathogenic yeast that is a human gut flora and the most common fungal pathogen causing the human candidiasis with symptoms of mouth thrush and vagina infection.[1-3] In the United States, candidemia is the fourth most common type of nosocomial bloodstream infection and is estimated to cause 2800 to 11200 deaths annually.[4,5] A mortality rate of 40% was reported for patients with systemic candidiasis due to *C. albicans*.[6]

Phosphodiesterases (PDEs) are unique enzymes decomposing cyclic adenosine and guanosine 3', 5'-monophoshophates (cAMP and cGMP).[7,8] For critical roles of the second messengers cAMP and cGMP in numerous physiological processes such as cardiovascular diseases,[9] inhibitors of human PDEs have been widely studied as therapeutics for treatment of human diseases.[7,8] The most successful example of this drug class is the PDE5 inhibitor sildenafil (Viagra) that has been approved for the treatment of male erectile dysfunction and pulmonary artery hypertension.[10,11]

Yeast genome contains two types of PDEs: yPDE1 and yPDE2. Yeast PDE1 belongs to the class II PDE superfamily and uses two zinc ions for its catalysis.[12] The sequence alignment shows that yPDE1 has a similar structure to the metalloproteins.[12,13] Indeed, the crystal structure of yPDE1 revealed its folding architecture comparable with those of metallo-β-lactamases.[14] Yeast PDE2 is a member of the class I PDE superfamily and shares a similar folding of its catalytic domain with human PDEs.[12]

Both yPDE1 and yPDE2 hydrolyze cAMP and participate in cAMP signaling pathways. Yeast PDE2 was named as high affinity cAMP PDE for their K_M values in a range of 0.17 to 1.0 μM,[15-17] whereas yPDE1 has low affinity with K_M of 100 - 150 μM for cAMP.[18-20] In contrast with the well characterized roles of cAMP in the physiological processes of yeast, the cGMP signaling pathway of yeasts has rarely been reported. *Candida albicans* PDE1 was reported to have K_M of 250 and 490 μM, and Vmax of 0.044 and 1.17 μmol/mg/min respectively for cGMP and cAMP,[21] suggesting its inefficiency in the cGMP signaling pathway due to its extremely low Vmax.

The cAMP signaling system has been shown to play critical roles in physiological processes of yeasts, including metabolism, cell wall biosynthesis, cell growth, and mating.[22-27] Overexpression of yPDE2 gene enhances the tolerance of yeast to oxidative and ethanol stresses for survival.[28-30] However, since no structures of any yeast PDE2s or their complexes with ligands are available to date, the cAMP signaling in physiological processes of yeasts have been poorly illustrated. Here, we report the enzymatic characterization and crystal structures of *Candida albicans* PDE2 (caPDE2) and its complex with non-selective inhibitor 3-isobutyl-1-methylxanthine (IBMX). These studies provide insight into the cAMP hydrolysis in yeast and the structural basis for design of caPDE2 inhibitors that could be new therapeutics for treatment of candidiasis.

Material and Methods

Protein expression and purification

The cDNA of the full-length human caPDE2 (residues 1-571) was subcloned into the expression vector pET28a, following the previously published protocol.[31] The resultant pET28-caPDE2 plasmid was confirmed by DNA sequencing and transferred into *E. coli* strain BL21 (CodonPlus) for overexpression. The *E. coli* cells carrying pET28-caPDE2 plasmid were grown in LB medium at 37°C to absorption of A600 = ~0.5 and then turn the shaker temperature down

to 12°C. When the shaker temperature reaches 12°C, 0.1 mM IPTG was added to induce overexpression of caPDE2 at 12°C for about 40 hours. Typical yield is about 5 g cell per liter culture. Harvested cells are centrifuged, weighed, and stored at −20°C for use.

The *E. coli* cells carrying caPDE2 were suspended in an extraction buffer of 20 mM Tris.base, pH 8.0, 0.3 M NaCl, 15 mM imidazole, 1 mM β-mercaptoethanol (4-8 ml buffer per gram of cell) and cleaved by ultrasonication or passing through Nano DeBee homogenizer at 20k psi. The recombinant caPDE2 protein was passed through a Ni-NTA column (Qiagen), subjected to thrombin cleavage, and further purified by Q-Sepharose and Superdex 200 columns (GE Healthcare). A typical purification batch yielded about 20 mg caPDE2 protein from 2 liters of cell culture. Purity of the proteins was estimated to be >95% by SDS polyacrylamide gels.

Crystallization and structure determination

The 10-15 mg/ml full length caPDE2 (1-571) was stored in a buffer of 20 mM Tris.base, pH 7.5, 50 mM NaCl, 1 mM β-mercaptoethanol, 1 mM EDTA. It was crystallized at room temperature by hanging drop against a well buffer of 50 mM MES, pH 6.5, 0.1 M ammonium sulfate, 6-10% PEG8000, or a buffer of 50 mM Na citrate pH 5.6, 0.1 M ammonium acetate, 5% glycerol, and 6-10% PEG3350. The unliganded caPDE2 has the space group C2 with unit cell dimensions of a = 139.5, b = 74.8, c = 65.5 Å, and β = 109.1°. The caPDE2-IBMX complex was prepared by soaking the native crystals in the crystallization buffer with 10 mM IBMX. A cryoprotectant was prepared by the crystallization buffer plus 20% glycerol and used to freeze the crystals. The diffraction data of the unliganded caPDE2 and its IBMX complex were collected at Shanghai Synchrotron Radiation Facility. The single-wave length anomalous diffraction data of native caPDE2 were collected at the zinc peak wavelength of 1.28149 Å on beamline ID22 of SERCAT at Advanced Photon Source of Argonne National Laboratory. All data were processed by program HKL2000.[32] The structure determination was first tried by molecular replacement program AMoRe,[33] using the wild type PDE4D2 as the initial model. This trial produced a partial model with R-free of 0.48 at 1.8 Å resolution after manual rebuilding by program COOT[34] and refinement by program REFMAC.[35] The partial structure was then used for phasing the structure by the MR-SAS module of PHENIX and automatic modeling by the AutoBuild module of PHENIX.[36] The PHENIX phasing yielded an R-free of 0.3 at 1.8 Å resolution and a traceable map. On basis of this map, the whole structure of full-length caPDE2 was manually built by COOT and finally refined by REFMAC to R-free of 23% (Table 1).

Table 1. Statistics on diffraction data and structure refinement

Data collection	caPDE2 native	caPDE2-IBMX	caPDE2 SAS data
Space group	C2	C2	C2
Unit cell (a, b. c, Å, β)	139.5, 74.8, 65.5, 109.1°	138.2, 73.6, 65.0, 108.5°	138.7, 73.9, 65.2 108.5°
Resolution (Å)	1.8	1.9	1.95
Wave length (Å)	1.0	1.0	1.28149
Unique reflections	57,843	47,636	86,446
Total measurements	423,455 (7.3 fold)	341,355 (7.2 fold)	646,099 (7.5 fold)
Completeness (%)	99.2 (98.9)*	97.4 (96.7)	96.5 (94.2)
Average I/σ	15.2 (4.4)*	14.5 (3.2)	10.1 (3.0)
Rmerge	0.067 (0.82)*	0.069 (0.80)	0.080 (0.68)
Structure Refinement			

R-factor	0.199	0.190	
R-free	0.226 (5.0%)‡	0.212 (5.0%)‡	
Resolution (Å)	65-1.8	65-1.9	
RMS deviation for			
Bond (Å)	0.007	0.005	
Angle	1.08°	0.98°	
Average B-factor (Å^2)			
Protein	34.6 (4276)§	36.4 (4208)§	
Inhibitor		68.5 (16)	
Zn	34.9 (1)	32.7 (1)	
Mg	26.7 (1)	27.4 (1)	
Water	34.0 (231)	37.7 (185)	
Remachandran Plot (%)			
Most favored	94.0	94.3	
Allowed	5.8	5.7	
Generally allowed	0.2		

*The numbers in parentheses are for the highest resolution shell.
‡The percentage of reflections omitted for calculation of R-free.
§The number of atoms in the crystallographic asymmetric unit.

Enzymatic properties

The enzymatic activities were assayed using ^{3}H-cAMP or ^{3}H-cGMP as substrate, as previously reported.[31] Briefly, the wild type proteins were incubated with a reaction mixture of 20 mM Tris.HCl, pH 7.5, 10 mM $MgCl_2$, 0.5 mM DTT, ^{3}H-cAMP or ^{3}H-cGMP (final concentration of 0.006 nM) at room temperature for 15 min. The reaction was terminated by addition of 0.2 M $ZnSO_4$. The reaction product ^{3}H-AMP or ^{3}H-GMP was precipitated out by addition of 0.2 N $Ba(OH)_2$ while unreacted ^{3}H-cAMP or ^{3}H-cGMP remained in the supernatant. Radioactivity in the supernatant was measured by a liquid scintillation counter. The steady state kinetic was followed to obtain K_M and kcat, which were calculated by non-linear regression. The inhibition of caPDE2 by the inhibitors of human PDEs was screened at a single concentration (10 μM) of the inhibitors. The IC_{50} of IBMX was measured at nine concentrations of IBMX and suitable concentrations of the enzymes.

Results

Monomeric caPDE2 structure

The structure of the full-length caPDE2 (amino acids 1-571) contains four parallel β-strands, twenty-six α-helices, and three 3_{10} helices (Fig. 1). Most parts of the structure have solid conformation, except for disorder of four loops: Asn54 – Thr76, Gly105 – Gly111, Cys142 – His155, and Asn325 – Glu330 (amino acids in cyan color, Fig. 1d). In comparison with human PDEs, the molecule of yeast caPDE2 can be divided into an N-terminal region (residues 1-201) and a C-terminal catalytic domain (202-571).

The crystallographic asymmetric unit contains a single molecule of caPDE2, which appears to form a monomer in the crystal form and may serve a catalytic unit of the enzyme in the biological system. This argument is supported by a monomeric form in liquid, as shown by a single peak at about 60 kDa from the molecular sieving column Superdex 200, which is in consistence with the calculated molecular weight of 65519 Daltons of full length caPDE2.

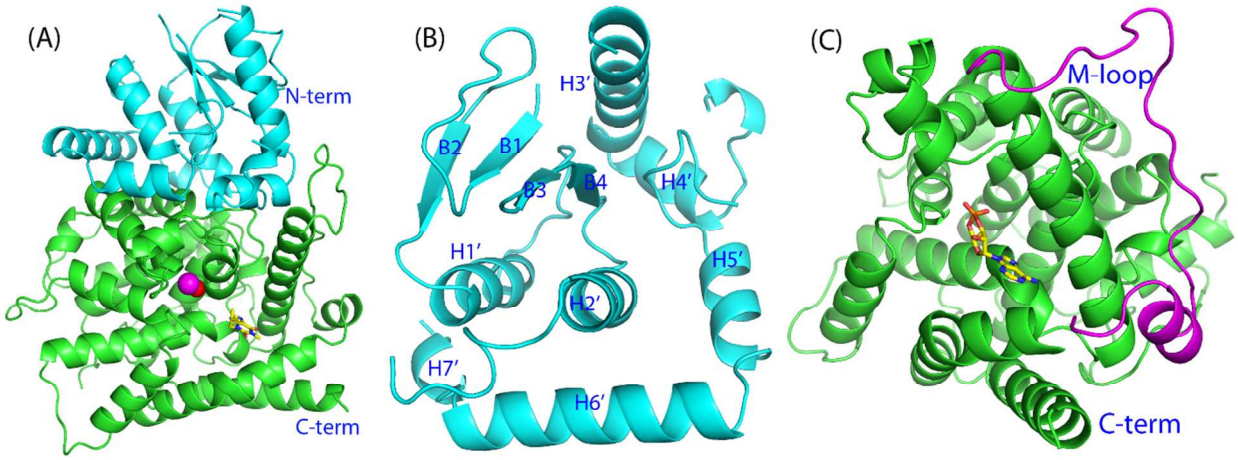

(D)

```
                B1                B2              H1′                B3
caPDE2     MAEVLSLVDLEIPQVTDKYYKFDTFKHLICHLFKKTSTETDSNVPIVIIFPTNNDIPSRK 60
                                                H2′        B4          H3′
caPDE2     TRSTTTTTTTTTTTTNTSKLDNLPFSDKSLLIQFFFTHLNILMIQGENSDEGKLYQEISSA 120
                     H4′                                        H5′   H6′
caPDE2     KELLTNRISRVGNWTGTTHFRYCRHENDCGLLNQHSKIAGIIPTMTYILNCNATRSEIAT 180
                          H7′
caPDE2     NQLIYLYRLMIEEINFIELLQ 201

caPDE2 202 DASTTRLSQLCYAVGHWSFPAHNLS--NDDLVYCVYLMIDYAIKQVEGFDNIPLNELLAF 259
PDE4D2  86 TEQEDVLAKELEDVNKWGLHVFRIAELSGNRPLTVIMHTIFQERDLLKTFKIPVDTLITY 145
                H1                H2              H3        H4        H5
                                  FKQFVEDPKLDYTEVHDKHTVLIALQNNSSEEK
caPDE2     IFIVRDTYKNGNPFHNFRHAVDVLQACFHFLIRLGSLPK*ASLNPIQTLGLLVAALGHDV 351
PDE4D2     LMTLEDHYHADVAYHNNIHAADVVQSTHVLLSTPALEAV---FTDLEILAAIFASAIHDV 202
                                  H6                        H7

caPDE2     GHPGTTNDFMIKFSAPTALLYNDRSVLESYHASLFINKVLRICWPDLLTCTIEEKSELTI 411
PDE4D2     DHPGVSNQFLINTNSELALMYNDSSVLENHHLAVGFKLLQEENCDIFQNLT--KKQRQSL 260
                | H8 H-loop H9 |        H10                       H11

caPDE2     RSLIISSILATDMGEHNEYVNRLKSFKTHNEIL-------NHDNTVKLISALLIKCADI 463
PDE4D2     RKMVIDIVLATDMSKHMNLLADLKTMVETKKVTSSGVLLLDNYSDRIQVLQNMVHCADL 319
                H11               H12                       H13

caPDE2                                        DLTYDDVPHELREILEI
caPDE2     SNVTRPLRVSAQWAMVLSREFAEVELLKSVIKKDIDLDFTK*QPDIHKGQIFFINLFAE 538
PDE4D2     SNPTKPLQLYRQWTDRIMEEFFRQGDRERERGMEISPMCDKHNASVEKSQVGFIDYIVH 378
                          H14             |     M-loop |   H15

caPDE2     NLFNSVSDL-LPQLQYTCDIIMENKLFWLERAKK 571
PDE4D2     PLWETWADLVHPDAQDILDTLEDNREWYQSTIPQ 412
           H15               H16
```

Fig. 1. Structure of caPDE2. (A) Ribbon presentation on the structure of full-length caPDE2. The cyan and green ribbons represent the N-terminal fragment and catalytic domain, respectively. The divalent metals of zinc and magnesium are shown as red and pink balls. IBMX is shown as yellow sticks. (B) Ribbon presentation of the N-terminal region of caPDE2 (residues 1-201). (C) Ribbon model of the catalytic domain of caPDE2. The pink coil is a fragment corresponding to the M-loop of PDE4D that plays important roles in binding of inhibitors. (D). Sequence alignment of caPDE2 to PDE4D2. The secondary structures are highlighted by colors of yellow for β-strands, green for α-helices, and cyan for 3_{10} helices. Letters H1 etc represent the helices in the PDE4D2 structures. The four metal binding residues are shown in red letters. Symbol * indicates the insertion of caPDE2 residues listed above.

Tight association of the N- and C-terminal domains into a rigid entity of caPDE2

The N-terminal region of caPDE2 contains 11 helices and 4 parallel strands (Fig. 1B) and assembles into a topology that does not resemble to a specific structural motif, as predict by program SMART (http://smart.embl-heidelberg.de/). However, a comparison of caPDE2 with known structures in the RCSB Protein Data Bank by program DALI[37] showed that the first 140 residues of caPDE2 have a folding comparable with several proteins. The best match is with the structures of the argonaute protein family that plays a central role in RNA silencing processes and binds different classes of small non-coding RNAs.[38] For example, the N-terminal fragment (1-140) of caPDE2 shares the folding topology with *Kluyveromyces polysporus* argonaute (PDE code of 4F1N, Z-score of 5.4 and RMSD of 3.4 for 94 residues) and human argonaute (5T7B, Z-score of 4.9 and RMSD of 3.7 for 102 residues). A superposition shows that the headpin of small guide RNA from the argonaute proteins apparently fits the shallow cavity in the N-terminal caPDE2. However, further experiments are required to verify if the small RNAs bind caPDE2 for a possible involvement of caPDE2 in other physiological processes.

A close examination of the caPDE2 structure reveals that the N-terminal region of caPDE2 is tightly associated with its catalytic domain via numerous hydrophobic and hydrophilic interactions on the interfaces between the helices of the N-terminus (H1', H4'- H7') and the C-terminus (H5, H9, H10, and H14, Fig. 2A). These massive interactions make the whole caPDE2 molecular looked like a rigid single domain. The assembly of caPDE2 is different from the structures of human PDEs, in which the N-terminal regions form an isolated domain and play roles in regulation of PDE catalysis or cross talk to other signaling systems.[7,8] The single domain of caPDE2 may imply that the N-terminal region would unlikely allosterically regulate the catalysis, although it is unknown how it involves in the catalysis. In addition, the rigid single domain of caPDE2 may mean stability of its molecular conformation, and thus favors taking environmental stresses without significant changes of conformation for biological functions. This argument is consistent with the observations that yeast PDE2 tolerates cold shock[28], oxidative [29] and alcoholunlikely stresses.[30]

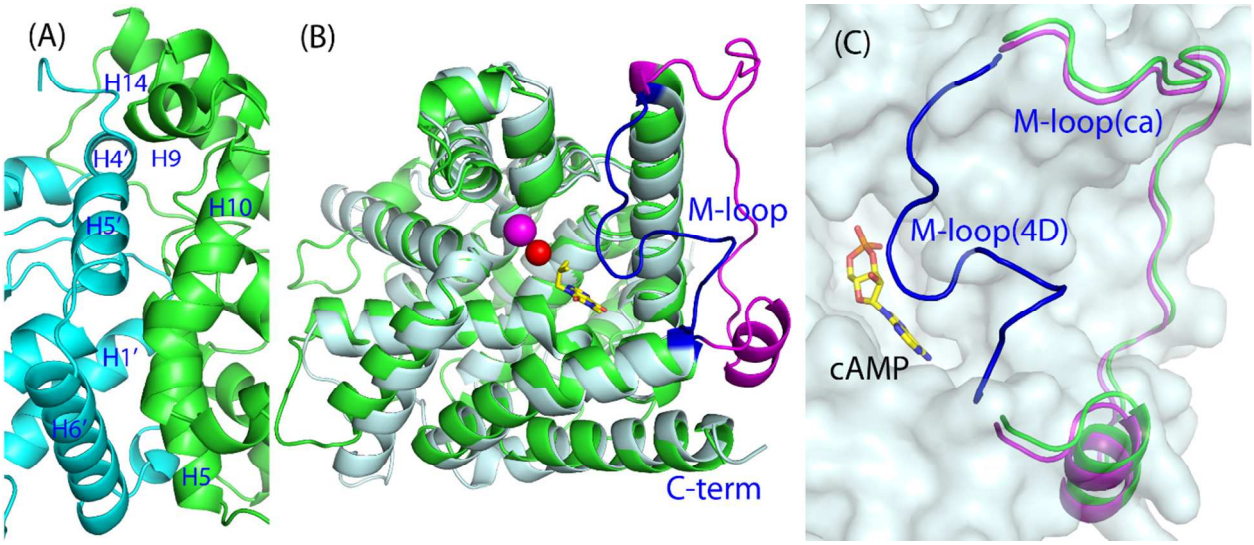

Fig. 2. Structural comparison of caPDE2 with human PDE4D. (A) Interface regions between the N- and C-terminal domains of caPDE2. The sequences can be found in Fig. 1D. (B) Ribbon model for the superposition between the catalytic domains of caPDE2 (green) and PDE4D2 (pale ribbons). The blue coil is the M-loop of PDE4D that plays important roles in binding of inhibitors and substrate. The corresponding loop of caPDE2 (purple) swings away from the active site and does not involve in substrate/inhibitor binding in the current conformation state. (C) Surface model on a close view of the location of the M-loops. The blue coil is the M-loop of PDE4D. Substrate cAMP is modeled from the superposition with the PDE4D-cAMP structure.[39]

Off-site of the M-loop may imply a different inhibitory mechanism of yeast from human

The C-terminal catalytic domain of caPDE2 contains pure helices and is well superimposed with the catalytic domain of PDE4D2 (Fig. 2B). The sequence alignment (Fig. 1D) shows that sixteen α-helices of PDE4D2 are conserved in the catalytic domain of caPDE2. However, caPDE2 has two insertions with residues of Phe299 to Ser333 and Lys496 to Asp524. The fragment of Phe299 to Ser333 has coil conformation without definitive secondary structures and is located at the back of the molecule, implying its less critical role in the catalysis. The fragment of Lys496 to Asp524 of caPDE2 corresponds to the coiled M-loop of PDE4D2 (residues Met352 - Val365 in PDE4D2), but contains an additional helix (Fig. 2B). The M-loops of human PDEs are located at an edge of the active site and shown to play a critical role in selective binding of substrates and inhibitors of human PDEs.[40] However, the corresponding fragment of caPDE2 swings away from the active site, leaving the binding pocket widely open (Figs. 2B & 2C). This fragment of caPDE2 is well ordered as shown by solid electron density in both (Fo-Fc) and (2Fo-Fc) maps, and has the same conformation in the structures of the unliganded caPDE2 and its IBMX complex, implying that IBMX binding does not promote the conformational changes. Since only residues Asp499-Asp501 of this fragment are involved in crystallographic lattice contacts with itself, the conformation of this fragment is unlikely to be impacted by the lattice contacts, but rather determined by massive interactions of the fragment with other residues within the same molecule. If a structure of caPDE2 in complex with a highly selective inhibitor has similar conformation to the unlignaded enzyme state, non-participation of the caPDE2 loop in the catalysis will be confirmed, thus implying a different mechanism for inhibitory regulation of the yeast PDE from human PDEs.

Conserved catalytic path of caPDE2

The catalytic domain of caPDE2 contains two divalent metals that were assigned as zinc and magnesium for their chelation with the same four invariant residues as human PDEs (Fig. 3): His278 (His164 of PDE4D2), His349 (His200), Asp350 (Asp201), and Asp462 (Asp318). The metal assignment is supported by the comparable B-factors of Zn and Mg (37 and 27 Å^2) with the average of protein atoms (34 Å^2, Table 1). This is also consistent with the early reports that bakery yeast PDE2 contained zinc ion and that magnesium ion yielded the highest hydrolytic activity.[18,19] The zinc ion has an octahedral conformation and forms four coordinations with protein residues of His278, His349, Asp350, and Asp462, and two waters (W1 and W2 in Fig. 3). The magnesium ion also has an octahedral conformation and chelates with Asp350 plus five water molecules. The water bridging two divalent metals (W1 in Fig. 3) may be a hydroxyl ion, as early proposed.[41]

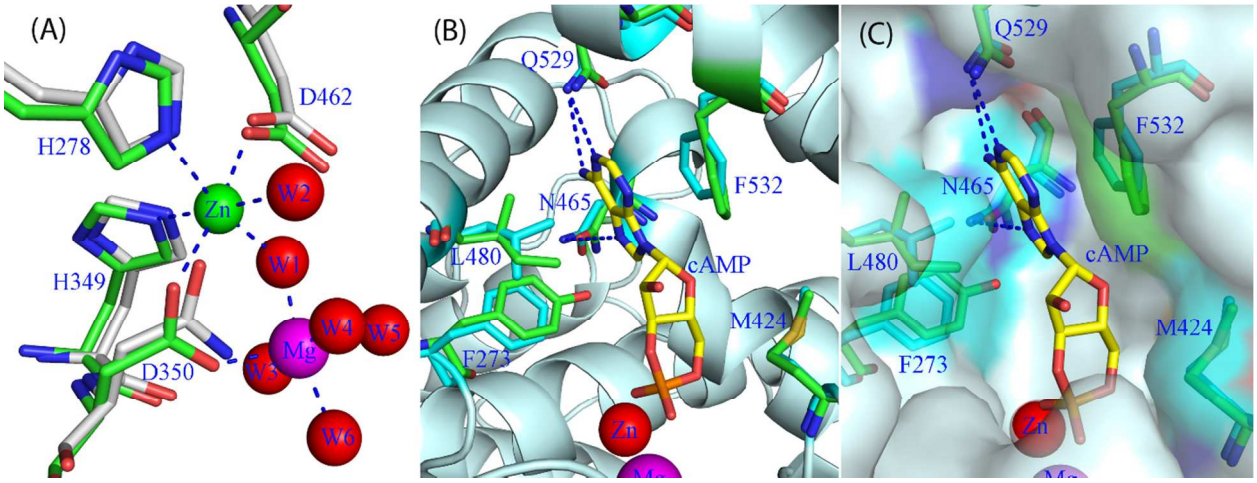

Fig. 3. Active site of caPDE2. (A) A comparison of the metal binding between caPDE2 (green sticks) and PDE4D2 (grey). Labels show caPDE2 residues. The superposition used the PDE4D D201N mutant in complex with cAMP. Zinc forms an octahedron with His278, His349, Asp350, Asp462, water (W2), and a hydroxyl ion (W1). The magnesium ion also has an octahedral conformation in coordination with Asp350 and five water molecules. (B) Model of substrate cAMP binding to caPDE2. Substrate cAMP was generated by the superposition between the structures of caPDE2 and the PDE4D2 D201N mutant. The caPDE2 residues are shown as green sticks and labeled. The corresponding residues of PDE4D are shown in cyan. (C) Surface model on cAMP binding.

To further explore the similarity of the yeast catalysis to human PDEs, caPDE2 is superimposed over the structure of PDE4D2 in complex with substrate cAMP.[39] The superposition reveals well conservation of most key residues at the active site (Fig. 3), including Phe273 (Tyr159 of PDE4D2), His274 (His160), His353 (His204), Leu480 (Ile336), Phe484 (Phe341), Gln529 (Gln369), and Phe532 (Phe372), as well as the four metal binding residues. The corresponding human PDE residues to His274, His353, and Gln529 of yeast caPDE2 were shown to play critical roles in either hydrolysis of substrates [39] or recognition of inhibitors.[40,42] The modeled cAMP fits well to the active site of caPDE2, in which the adenosine ring forms hydrogen bonds with invariant Gln529 and stacks against conserved Phe532 (Fig. 3). These interactions would orient the phosphate portion of cAMP toward the motel pocket for hydrolysis. We proposed a mechanism of nucleophilic attack for the cAMP conversion by PDE4D2,[41] which

would also applied to the hydrolysis of cAMP by caPDE2. In short, the first step of the catalysis would be the activation of the bridging water/hydroxyl ion by negatively charged carboxyl head of Asp462, a zinc chelating residue. The second step would be the nucleophilic attack on the phosphor atom of cAMP by the hydroxyl ion and may temporarily form a transition state in which the phosphor atom contains intermediate six covalent bonds. The last step would be the donation of a proton from His274 to produce product AMP.

Binding of IBMX induces local conformation changes

The structure of caPDE2-IBMX shows that non-selective inhibitor IBMX fits into the hydrophobic slot of caPDE2 with stacking against Phe532 on one side and interacting with hydrophobic residues of Leu480 and Phe484 on another side. In addition, IBMX forms two hydrogen bonds with the invariant Gln529 and Asn465. The superposition of the caPDE2-IBMX complex over the unliganded caPDE2 structure reveals no significant changes on the positions and conformations of most residues of the proteins, including the metal binding residues. However, the side chains of Asn465 and Phe484 are undergone dramatic conformational changes in order to form the hydrogen bond and hydrophobic interactions with IBMX (Fig. 4). The butanyl group of IBMX is disordered in the crystal structure.

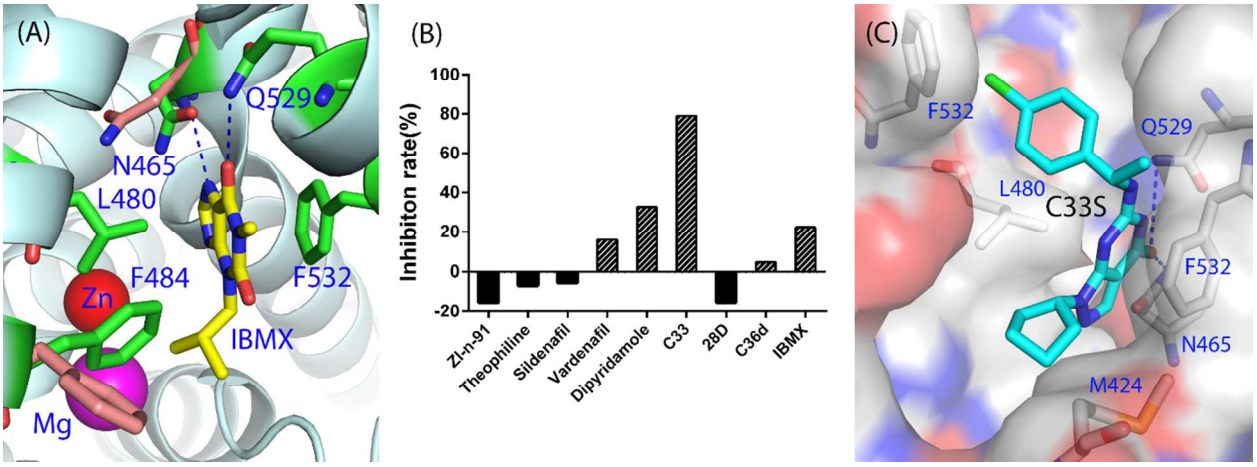

Fig. 4. Inhibition of caPDE2. (A) Binding of IBMX. IBMX fits into the hydrophobic slot of caPDE2 (Leu480, Phe484, and Phe532) and forms two hydrogen bonds with Asn465 and Gln529 (dotted lines). IBMX binding causes dramatic changes of the side chain conformations of Asn465 and Phe484 (salmon sticks for the unliganded caPDE2 and green for caPDE2-IBMX). (B) Inhibition of caPDE2 by human PDE inhibitors at 10 μM concentration, except for 200 μM IBMX. Inhibitors plotted are Zl-n-91 (PDE4), IBMX and theophylline (non-selective), sildenafil and vardenafil (PDE5), dipyridamole (PDE3 and PDE5), C33, 28D and C36D (PDE9). (C) Docking of PDE9 inhibitor C33S to caPDE2.

The binding pattern of IBMX in caPDE2 is similar to those observed in PDE4D,[31] PDE8A,[43] and PDE9A,[44] in terms of hydrogen bonding and hydrophobic interaction, although the detailed orientations are different. Since the hydrophobic stacking against a conserved phenylalanine and hydrogen bonding with invariant glutamine are essential for binding of most PDE inhibitors,[40] the IBMX binding could be used as a template for design of selective yeast inhibitors.

caPDE2 has the highest affinity with cAMP

The full length yeast caPDE2 has K_M of 35 nM and k_{cat} of 0.16 s^{-1} for substrate cAMP and K_M of 880 μM and k_{cat} of 0.031 s^{-1} for cGMP. The substrate specificity of k_{cat}/K_M^{cAMP} over k_{cat}/K_M^{cGMP} is 1.32 x 10^5 (Table 2), indicating that caPDE2 is highly cAMP specific and does not hydrolyze cGMP under normal physiological conditions. Our K_M of 35 nM is basically comparable 100 to 200 nM for bakers' yeast PDE2,[15,20,45] but much smaller than the K_M values of 1.5, 0.2, 1.8 μM of cAMP-specific PDE4D2, PDE7A1, and PDE8A (Table 2).[31,43] The explanation was not clear, but the replacement of the tyrosine (Tyr159 of PDE4D2), which is absolutely sonserved in human PDEs, with Phe273 of caPDE2, would make tighter hydrophobic interactions with adenosine of cAMP (Fig. 3) and thus enhance cAMP binding. However, explanation to the inability of caPDE2 in hydrolysis of cGMP is unknown. Careful overlay of three structures: caPDE2, PDE4d-cAMP, and PDE9A-cGMP showed that substrates cAMP and cGMP have similar conformations and interact with a set of active site residues that are mostly conserved in the structures of PDE4D-cAMP and PDE9-cGMP. It is not obvious which element, amino acid variation or minor conformation change, determines the selectivity of cAMP versus cGMP. It is also unclear how much the M-loops contributes to the differention of the cAMP/cGMP binding. The M-loop is a integral part of the active sites and shows the largest conformation changes in human PDEs, and apparently plays an important role in substrate binding of human PDEs. Moving away of the M-loop in caPDE2 revokes its role in the catalysis and might weaken the cGMP binding.

Table 2. Kinetic parameters of caPDE2 (reference 36)

Enzymes	K_M^{cAMP} (μM)	k_{cat}^{cAMP} (sec^{-1})	$(k_{cat}/K_M)^{cAMP}$ ($s^{-1}\mu M^{-1}$)	K_M^{cGMP} (mM)	k_{cat}^{cGMP} (sec^{-1})	$(k_{cat}/K_M)^{cGMP}$ ($s^{-1}\mu M^{-1}$)	$(k_{cat}/K_M)^{cAMP}/(k_{cat}/K_M)^{cGMP}$
caPDE2 (1-571)	0.035 ± 0.004	0.163 ± 0.003	4.7	0.88 ± 0.18	0.031 ± 0.006	3.6 x 10^{-5}	132 x 10^3
PDE4D2 (1-507)	1.5 ± 0.2	3.9 ± 0.3	2.6	1.0 ± 0.1	5.2 ± 0.8	5.2 x 10^{-3}	500
PDE7A1 (130-482)	0.2±0.03	1.6±0.2	8.0	3.9 ± 0.7	6.8 ± 1.3	1.7 x 10^{-3}	4700
PDE8A1 (480-820)	1.8 ± 0.1	4.0 ± 0.1	2.2	1.6 ±0.1	1.6 ± 0.2	1.0 x 10^{-3}	2200

Screening on a few of selective or non-selective inhibitors of human PDEs showed that yeast caPDE2 is not significantly inhibited by the human PDE inhibitors (Fig. 4B), except for PDE9 selective inhibitor C33S,[46] which inhibited 79% activity of caPDE2 at 10 μM concentration. Dipyridamole at 10 μM, an anti-blood coagulator and inhibitor of PDE3 and PDE5 [47] inhibited 32% activity of caPDE2. The fit of the large dipyridamole to the caPDE2 active site is apparently due to moving away of the M-loop from the active site of caPDE2. IBMX, a common non-selective inhibitor of human PDEs, did not significantly inhibit caPDE2, as shown by 22% inhibition at 0.2 mM IBMX (Fig. 4B) and had IC_{50} of 0.96 mM, but surprisingly bound caPDE2 with a similar pattern as those in human PDEs.

Discussion

Conservation of fungal PDE2s

While numerous structures of human PDEs are available for design of inhibitors for treatment of human diseases, no structure of yeast PDE2 has been reported, leaving the functional mechanism for fungal PDE2 illusive. In a sense that secondary structures of proteins can be reliably predicted from sequences, the secondary structures of 18 fungal PDE2s were predicted by program PSIPRED (http://bioinf.cs.ucl.ac.uk/psipred/) and aligned to the crystal structure of caPDE2. The alignment showed that the secondary structures of the 18 fungal PDE2 are conserved (supplementary Fig. S1), implying that they may assemble into similar three dimentional structures as caPDE2 does. In addition, the residues interacting with divalent metals, substrates, or inhibitors (marked with * in Fig. S1) are almost invariant, suggesting a common mechanism for the catalysis of fungal PDE2s. Especially, Phe273 of caPDE2, which is absolutely conserved in all fungal PDE2s (Fig. S1) and corresponds to a tyrosine of all human PDEs (supplementary Fig. S2), might enhance hydrophobic interaction with cAMP as discussed above, implying a characteristic cAMP hydrolysis of fungal PDE2s.

It is interesting to note that caPDE2 has about 20 amino acid insertion in the M-loop (Fig. 1D) and many of other fungal PDE2s even have longer insertions (Fig. S1). The M-loops of human PDEs form an edge of the inhibitor binding pocket, have a similar size (supplementary Fig. S2) but different conformations, and play important roles for binding of substrate and inhibitors.[40] In contrast, the corresponding fragment of caPDE2 move away from the active site, suggesting its less critical role in the catalysis. It is unclear whether the M-loop fragments of other fungal PDE2 can move back to the active site. However, it might be difficult to fit a large fragment to the pocket that has a limited size. Further experiments are required to clarify this question.

Conclusion

Yeast cAMP-specific caPDE2 forms a rigid single domain of the molecule, in contrast with separate N- and C-terminal domains of human PDEs, implying a capacity of yeast PDE2 to resist environmental stresses. The different location of the M-loop of caPDE2 from human PDEs suggests a distinct inhibitory mechanism of caPDE2. This structure information may be useful for design of caPDE2 selective inhibitors for treatment of candidiasis.

Accession codes The coordinates and structural factors of the unliganded caPDE2 and its IBMX complex have been deposited into the RCSB Protein Data Bank with accession codes of 6CPT and 6CPU.

Acknowledgements We thank Shanghai Synchrotron Radiation Facility and beamline ID22 of SERCAT at Advanced Photon Source of Argonne National Laboratory for collection of the diffraction data. This work was supported in part by NIH GM59791 to HK, the National Natural Science Foundation of China (31471626, 31291944, YW), and the Intramural Research Program of NIEHS (H.W.).

Conflict of interests

The authors declare that they have no conflicts of interest with the contents of this article.

Supporting information:

Sequence alignment of 18 fungal PDE2s (Fig. S1)

Sequence alignment of the core catalytic domain of caPDE2 to human PDEs (Fig. S2).

References

1. Lass-Florl, C. (2009) The changing face of epidemiology of invasive fungal disease in Europe. *Mycoses 52*, 197–205.
2. Erdogan, A., and Rao, S. S. (2015) Small intestinal fungal overgrowth. *Curr Gastroenterol Rep*. *17*, 16.
3. Gow, N.A.R. (2017) Microbe Profile: Candida albicans: a shape-changing, opportunistic pathogenic fungus of humans. *Microbiology*. *163*, 1145–1147.
4. Bustamante, C. I. (2005) Treatment of Candida infection: a view from the trenches. *Curr. Opin. Infect. Dis*. *18*, 490–495.
5. Pfaller, M. A., and Diekema, D. J. (2007) Epidemiology of Invasive Candidiasis: A Persistent Public Health Problem. *Clin. Microbiol. Rev. 20*, 133–163.
6. Singh, R., Chakrabarti, A. (2017) "Invasive candidiasis in the southeast-Asian region". In prasad, rajendra, candida albicans: cellular and molecular biology, 2nd Ed. Switzerland, Springer International Publishing AG. p. 27.
7. Conti, M., and Beavo, J. (2007) Biochemistry and physiology of cyclic nucleotide phosphodiesterases: Essential components in cyclic nucleotide signaling. *Ann. Rev. Biochem*. *76*, 481-511.
8. Maurice, D. H., Ke, H., Ahmad, F., Wang, Y., Chung, J., and Manganiello, V. C. (2014) Advances in targeting cyclic nucleotide phosphodiesterases. *Nat. Rev. Drug Discov*. *13*, 290-314.
9. Kokkonen, K., and Kass, D. A. (2017) Nanodomain Regulation of Cardiac Cyclic Nucleotide Signaling by Phosphodiesterases. *Annu. Rev. Pharmacol. Toxicol*. *57*, 455-479.
10. Rotella, D. P. (2002) Phosphodiesterase 5 inhibitors: current status and potential applications. *Nat. Rev. Drug Discov*. *1*, 674–682.
11. Galie, N., Ghofrani, H. A., Torbicki, A., Barst, R. J., Rubin, L. J., Badesch, D., Fleming, T., Parpia, T., Burgess, G., Branzi, A., Grimminger, F., Kurzyna, M., and Simonneau, G. (2005) Sildenafil citrate therapy for pulmonary arterial hypertension. *N. Engl. J. Med*. *353*, 2148-2157.
12. Wentzinger, L., and Seebeck, T. (2007) Protozoal phosphodiesterases in *Cyclic nucleotide phosphodiesterases in health and disease*. Eds Beavo JA, Francis SH, and Houslay MD (CRC Press, Boca Raton, Florida), pp 277-300.
13. Bebrone, C. (2007) Metallo-beta-lactamases (classification, activity, genetic organization, structure, zinc coordination) and their superfamily. *Biochem. Pharmacol. 74*, 1686-1701.
14. Tian, Y., Cui, W., Huang, M., Robinson, H., Wan, Y., Wang, Y., and Ke, H. (2014) Dual specificity and novel structural folding of yeast phosphodiesterase-1 for hydrolysis of second messengers cyclic adenosine and guanosine 3',5'-monophosphate. *Biochem*. *53*, 4938-4945.
15. Suoranta, K., and Londesborough, J. (1984) Purification of intact and nicked forms of a zinc-containing, Mg2+-dependent, low Km cyclic AMP phosphodiesterase from bakers' yeast. *J. Biol Chem. 259*, 6964-6971.
16. Suoranta, K., and Londesborough, J. (1985) The specificity of yeast low-Km cyclic AMP phosphodiesterase towards free bivalent metal ions and the diastereoisomers of cyclic adenosine phosphorothioate. *Biochem. J. 226*, 897-900.

17. Sass, P., Field, J., Nikawa, J., Toda, T., and Wigler, M. (1986) Cloning and characterization of the high-affinity cAMP phosphodiesterase of Saccharomyces cerevisiae. *Proc. Natl. Acad. Sci. USA 83*, 9303-9307.
18. Londesborough, J., and Lukkari, T. (1980) The pH and temperature dependence of the activity of the high *K,* Cyclic Nucleotide Phosphodiesterase of Bakers' Yeast. *J. Biol. Chem. 255*, 9262-9267.
19. Londesborough, J., and Suoranta, K. (1983) The zinc-containing high Km cyclic nucleotide phosphodiesterase of bakers' yeast. *J. Biol. Chem. 258*, 2966-2972.
20. Uno, I., Matsumoto, K., and Ishikawa, T. (1983) Characterization of a cyclic nucleotide phosphodiesterase-deficient mutant in yeast. *J. Biol. Chem*. *258*, 3539-3542.
21. Hoyer, L. L., Cieslinski, L. B., McLaughlin, M. M., Torphy, T. J., Shatzmanl, A. R., and Livil, G. P. (1994) A *Candida albicans* cyclic nucleotide phosphodiesterase: cloning and expression in *Saccharomyces cerevisiae* and biochemical characterization of the recombinant enzyme. *Microbiol. 140,* 1533-1542.
22. Thevelein, J. M., Cauwenberg, L., Colombo, S., De Winde, J. H., Donation, M., Dumortier, F., Kraakman, L., Lemaire, K., Ma, P., Nauwelaers, D., Rolland, F., Teunissen, A., Van Dijck, P., Versele, M., Wera, S., and Winderickx, J. (2000) Nutrient-induced signal transduction through the protein kinase A pathway and its role in the control of metabolism, stress resistance, and growth in yeast. *Enzyme. Microb. Technol*. *26,* 819-825.
23. Jung, W. H., and Stateva, L. (2003) The cAMP phosphodiesterase encoded by CaPDE2 is required for hyphal development in *Candida albicans*. *Microbiol. 149,* 2961-2976.
24. Jung, W. H., Warn, P., Ragni, E., Popolo, L., Nunn, C. D., Turner, M. P., and Stateva, L. (2005) Deletion of PDE2, the gene encoding the high-affinity cAMP phosphodiesterase, results in changes of the cell wall and membrane in *Candida albicans. Yeast 22,* 285–294.
25. Bahn, Y. S., Staab, J., and Sundstrom, P. (2003) Increased high-affinity phosphodiesterase PDE2 gene expression in germ tubes counteracts CAP1-dependent synthesis of cyclic AMP, limits hypha production and promotes virulence of *Candida albicans*. *Mol. Microbiol. 50,* 391–409.
26. Wilson, D., Tutulan-Cunita, A., Jung, W. H., Hauser, N. C., Hernandez, R., Williamson, T., Piekarska, K., Rupp, S., Young, T., and Stateva, L. (2007) Deletion of the high affinity cAMP phosphodiesterase encoded by PDE2 affects stress responses and virulence in *Candida albicans*. *Mol. Microbiol. 65,* 841–856.
27. Wilson, D., Fiori, A., Brucker, K. D., Dijck, P. V., and Stateva L. (2010) *Candida albicans* Pde1p and Gpa2p comprise a regulatory module mediating agonist-induced cAMP signalling and environmental adaptation. *Fungal Genet. Biol. 47,* 742-752.
28. Park, J. I., Grant, C. M., and Dawes, I. W. (2005) The high-affinity cAMP phosphodiesterase of *Saccharomyces cerevisiae* is the major determinant of cAMP levels in stationary phase: involvement of different branches of the Ras–cyclic AMP pathway in stress responses. *Biochem. Biophys. Res. Commun. 327*, 311–319.
29. Drobna, E., Gazdag, Z., Culakova, H., Dzugasova, V., Gbelska, Y., Pesti, M., and Subik, J. (2012) Overexpression of the YAP1, PDE2, and STB3 genes enhances the tolerance of yeast to oxidative stress induced by 7-chlorotetrazolo[5,1-c]benzo[1,2,4]triazine. *FEMS Yeast Res*. *12*, 958-968.

30. Avrahami-Moyal, L., Braun, S., and Engelberg, D. (2012) Overexpression of PDE2 or SSD1-V in Saccharomyces cerevisiae W303-1A strain renders it ethanol-tolerant. *FEMS Yeast Res*. *12*, 447-455.
31. Wang, H., Liu, Y., Chen, Y., Robinson, H., and Ke, H. (2005) Multiple elements jointly determine inhibitor selectivity of cyclic nucleotide phosphodiesterases 4 and 7, *J. Biol. Chem*. *280*, 30949-30955.
32. Otwinowski, Z. and Minor, W. (1997) Processing of X-ray diffraction data collected in oscillation mode, *Methods Enzymol*. *276*, 307-326.
33. Navaza, J. and Saludjian, P. (1997) AMoRe: an automated molecular replacement program package, *Methods Enzymol*. *276*, 581-594.
34. Emsley, P., Lohkamp, B., Scott, W.G., and Cowtan, K. (2010) Features and development of Coot, *Acta Cryst. 66*, 486-501.
35. Winn, M.D., Murshudov, G.N., and Papiz, M.Z. (2003) Macromolecular TLS refinement in REFMAC at moderate resolutions, *Method Enz. 374*, 300-321.
36. Adams, P. D., Afonine, P. V., Bunkóczi, G., Chen, V. B., Davis, I. W., Echols, N., Headd, J. J., Hung, L. W., Kapral, G. J., Grosse-Kunstleve, R. W., McCoy, A. J., Moriarty, N. W., Oeffner, R., Read, R. J., Richardson, D. C., Richardson, J. S., Terwilliger, T. C., and Zwart, P. H. (2010) PHENIX: a comprehensive Python-based system for macromolecular structure solution. *Acta Cryst. D*. *66*, 213-221.
37. Holm, L., and Laakso, L.M. (2016) Dali server update. *Nucleic Acids Res*. 44(W1), W351-W344.
38. Hutvagner, G., and Simard, M. J. (2008) Argonaute proteins: key players in RNA silencing. *Nat Rev. Mol. Cell Biol*. *9*, 22–32.
39. Wang, H., Robinson, H., and Ke, H. (2007) The molecular basis for recognition of different substrates by phosphodiesterase families 4 and 10. *J. Mol. Biol. 371*, 302-307.
40. Ke, H. and Wang, H. (2007) Crystal structures of phosphodiesterases and implications on substrate specificity and inhibitor selectivity, *Curr. Top. Med. Chem*. *7*, 391-403.
41. Huai, Q., Wang, H., Sun, Y., Kim, H.Y., Liu, Y., and Ke, H. (2003) Three dimensional structures of PDE4D in complex with roliprams and implication on inhibitor selectivity, *Structure 11*, 865-873.
42. Card, G. L., England, B. P., Suzuki, Y., Fong, D., Powell, B., Lee, B., Luu, C., Tabrizizad, M., Gillette, S., Ibrahim, P. N., Artis, D. R., Bollag, G., Milburn, M. V., Kim, S. H., Schlessinger, J., and Zhang, K.Y. (2004) Structural basis for the activity of drugs that inhibit phosphodiesterases, *Structure 12*, 2233-2247.
43. Wang, H., Yan, Z., Yang, S., Cai, J., Robinson, H., and Ke, H. (2008) Kinetic and Structural Studies of Phosphodiesterase-8A and Implication on the Inhibitor Selectivity, *Biochem. 47*, 12760-12768.
44. Huai, Q., Wang, H., Zhang, W., Colman, R., Robinson, H., and Ke, H. (2004) Crystal structure of phosphodiesterase 9 shows orientation variation of inhibitor 3-isobutyl-1-methylxanthine binding. *Proc. Natl. Acad. Sci. USA*, *101*, 9624-9629.
45. Michaeli, T., Bloom, T. J., Martins, T., Loughney, K., Ferguson, K., Riggs, M., Rodgers, L., Beavo, J. A., and Wigler M. (1993) Isolation and characterization of a previously undetected human cAMP phosphodiesterase by complementation of cAMP phosphodiesterase-deficient Saccharomyces cerevisiae. *J. Biol. Chem*. *268*, 12925-12932.
46. Huang, M., Shao, Y., Hou, J., Cai, W., Liang, B., Huang, Y., Li, Z., Wu, Y., Zhu, X., Liu, P., Wan, Y., Ke, H., and Luo, H. B. (2015) Structural Asymmetry of Phosphodiesterase-

9A and a Unique Pocket for Selective Binding of a Potent Enantiomeric Inhibitor. *Mol Pharmacol. 88*, 836-845.

47. Gresele, P., Momi, S., and Falcinelli, E. (2011) Anti-platelet therapy: phosphodiesterase inhibitors. *Br J Clin Pharmacol*. *72*, 634-646.